

Probing localization effects in $\text{Li}_{0.9}\text{Mo}_6\text{O}_{17}$ purple bronze: An optical-properties investigation

J. Choi and J. L. Musfeldt

Department of Chemistry, University of Tennessee, Knoxville, Tennessee 37996, USA

J. He

Department of Physics, The University of Tennessee, Knoxville, Tennessee 37996, USA

R. Jin

Oak Ridge National Laboratory, P.O. Box 2008, Oak Ridge, Tennessee 37831, USA

J. R. Thompson and D. Mandrus

*Department of Physics, The University of Tennessee, Knoxville, Tennessee 37996, USA
and Oak Ridge National Laboratory, P.O. Box 2008, Oak Ridge, Tennessee 37831, USA*

X. N. Lin, V. A. Bondarenko, and J. W. Brill

Department of Physics and Astronomy, University of Kentucky, Lexington, Kentucky 40506, USA

(Received 11 September 2003; published 27 February 2004)

We report the polarized reflectance and optical conductivity of the quasi-one-dimensional conductor $\text{Li}_{0.9}\text{Mo}_6\text{O}_{17}$ as a function of temperature. The compound displays an unusual (non-Drude-type) mobile carrier response at low-energy, with partially screened vibrational features along the highly conducting b axis. In addition, we observe Mo $d \rightarrow d$ transitions near 0.42, 0.57, and 1.3 eV, and an O $p \rightarrow$ Mo d charge-transfer band near 4 eV. Perpendicular to the b axis, $\text{Li}_{0.9}\text{Mo}_6\text{O}_{17}$ exhibits semiconducting behavior with an optical gap of 0.4 eV and electronic structure similar to that of the b axis at higher energies. The substantial temperature dependence of the vibrational modes in this direction reveals that the lattice of $\text{Li}_{0.9}\text{Mo}_6\text{O}_{17}$ is not rigid. However, no noticeable change in the lattice through the 25 K metal-insulator transition is observed. Comparing x-ray and infrared data for several model materials, we establish an upper bound on the size of any lattice distortion in $\text{Li}_{0.9}\text{Mo}_6\text{O}_{17}$. Based upon these combined results, we argue that localization effects dominate the bulk and microscopic properties of this material.

DOI: 10.1103/PhysRevB.69.085120

PACS number(s): 71.30.+h, 71.45.Lr, 78.30.-j, 78.40.-q

I. INTRODUCTION

The low-dimensional conductor $\text{Li}_{0.9}\text{Mo}_6\text{O}_{17}$ (Li purple bronze) was extensively studied in the 1980s following the discovery of superconductivity at 2 K and an associated metal-insulator transition near 25 K.^{1,2} The metal-insulator transition appears as a resistivity upturn and was proposed to be due to a charge-density wave (CDW) distortion.³ As a consequence, Li purple bronze attracted attention as a CDW superconductor,^{4,5} which is of interest because competing density wave and superconducting states could be stabilized by application of pressure or magnetic field. The 2 K superconducting transition was quickly confirmed,^{3,6} but the nature of the 25 K metal-insulator transition is an ongoing puzzle.^{3,6-19}

Four different models have been proposed to describe the 25 K transition in $\text{Li}_{0.9}\text{Mo}_6\text{O}_{17}$: CDW, spin-density wave, localization, and Luttinger liquid.^{3,6-18} In the CDW scenario, electron-phonon coupling induces a distortion and opens a gap at the Fermi surface. As described below, much (but not all) of the experimental evidence points in this direction.^{3,8,9,19} Spin-density wave models require a characteristic shape and an anisotropic drop in the susceptibility at 25 K which is not observed, and existing localization models require strong disorder effects that would seem to preclude low-temperature superconductivity. Neither model captures

the essential characteristics of the material. Evidence for an alternate, perhaps Luttinger liquid state above 25 K comes mainly from selected photoemission studies,¹¹⁻¹⁸ the absence of an optical gap,²⁰ and arguments that $\text{Li}_{0.9}\text{Mo}_6\text{O}_{17}$ is a correlated (rather than classical) quasi-one-dimensional metal at low temperature. Among the distinguishing characteristics of a Luttinger liquid are low-dimensionality, strong electron correlation, spin-lattice-charge separation, peaks in the spectral function, and zero conductance at low temperature.²¹⁻²⁶

Among the aforementioned models, the CDW scenario of the 25 K transition is widely supported by the physical-properties investigations,¹⁹ although there are important holes in this picture, as described below. The transport data present an especially compelling case for the CDW superconductor model in $\text{Li}_{0.9}\text{Mo}_6\text{O}_{17}$.^{3,8,9,19} Pressure stabilizes the superconducting state, whereas it suppresses the 25 K transition above 12 kbar.⁹ This effect has been associated with an increased density of states at the Fermi level with pressure. In contrast, an applied magnetic field suppresses T_c .²⁷ The inverse correlation between the superconducting transition temperature and the metal-insulator transition is consistent with a CDW instability taking place at 25 K. The thermopower of $\text{Li}_{0.9}\text{Mo}_6\text{O}_{17}$ is holelike, with a decrease below 25 K.⁸ The Hall effect also shows a drop in the number of carriers, but it indicates a mobility increase in the low-

temperature phase.¹⁹ The heat capacity displays a broad feature at 25 K that was interpreted as evidence for a thermodynamic transition.³ A $0.45b^*$ nesting vector was predicted for $\text{Li}_{0.9}\text{Mo}_6\text{O}_{17}$,¹⁰ and the slight band dispersion in the transverse direction suggests that incomplete nesting is possible.^{30,31} A portion of the recent photoemission work is also consistent with the CDW picture of the 25 K metal-insulator transition,^{16–18} and a far-infrared density wave gap ($2\Delta \sim 80$ meV) has been extracted from the results.¹⁷ At base temperatures, $\text{Li}_{0.9}\text{Mo}_6\text{O}_{17}$ is a BCS superconductor, with $H_{c2} = 0.85$ T, coherence length $\xi = 194$ Å, and $\Delta = 0.45$ meV in the b direction;³ the superconducting carriers are thought to condense from the remaining (unnested) parts of the Fermi surface.

From the evidence in the preceding paragraph, it may appear that the case for the CDW mechanism is strong. There are, however, several open problems. One of the most important manifestations of a CDW transition is a structural distortion concomitant with the metal-insulator transition.³² Such a structural change provides direct evidence of CDW formation.³³ The structure of $\text{Li}_{0.9}\text{Mo}_6\text{O}_{17}$ is typical of many low-dimensional transition metal oxides, consisting of four MoO_6 octahedra and two MoO_4 tetrahedra per unit cell. Along the conducting b axis, two Mo^{5+} atoms in neighboring MoO_6 octahedra form double zigzag chains together with their corner sharing axial oxygens between them.³⁴ Note that the structure of $\text{Li}_{0.9}\text{Mo}_6\text{O}_{17}$ is quite different from the more two-dimensional Na, K, and Tl purple bronzes,^{35–37} all of which indisputably display CDW transitions.¹⁹ Despite extensive efforts, no lattice instability has been found in $\text{Li}_{0.9}\text{Mo}_6\text{O}_{17}$ near 25 K.³⁸ There are two ways to interpret these results: (1) there is no structural distortion or (2) the structural distortion is extremely weak and below the sensitivity of the best experimental work at this time. The lack of a clear structural instability is the major motivation for invoking an alternate model of the 25 K metal-insulator transition. The optical properties of $\text{Li}_{0.9}\text{Mo}_6\text{O}_{17}$ also diverge from what is expected for a CDW material.²⁰ Degiorgi *et al.* report temperature-independent vibrational properties, with no evidence for a lattice distortion at 25 K.²⁰ In addition, no optical gap was observed at low temperature. Instead, the low-energy dynamics were interpreted with a Drude model, assuming a free-carrier response over the full temperature range.²⁰ These results spurred additional electronic structure work, especially in the area of photoemission. However, the photoemission results are controversial because different investigations point variously towards either CDW or Luttinger liquid behavior.^{11–18} Certainly, the aforementioned optical-properties work combined with selected photoemission studies^{11–15} suggest that the CDW channels may be blocked, and demand that other models of the 25 K metal-semiconductor transition be considered. Recent electronic structure calculations also point toward the importance of electron correlation in this systems.³⁰

In order to address continuing questions on the dynamics of this prototypical quasi-one-dimensional material and provide additional information about the 25 K transition, we investigated the variable temperature polarized reflectance

and optical conductivity spectra of $\text{Li}_{0.9}\text{Mo}_6\text{O}_{17}$. In so doing, we find an unusual mobile carrier response at low energies, evidence for a nonrigid lattice, and reason to reassess the optical excitations based upon new electronic structure calculations and photoemission results.^{12,30,31} Despite the temperature dependence of the vibrational properties and our careful search for indirect evidence of a structure modification at 25 K, we do not find any noticeable change in the lattice through the 25 K metal-insulator transition. Therefore, if this transition is of charge-density wave type, the distortion is extremely small. Considering the significant influence of the previous optical-properties study of Li purple bronze, we also present a more complete view of the variable temperature dynamics and an analysis of the optical conductivity, both of which point toward localization as the dominant effect in this material.

II. EXPERIMENT

Single crystals of $\text{Li}_{0.9}\text{Mo}_6\text{O}_{17}$ were grown using the temperature gradient flux method, as described by McCarroll and Greenblatt.² Appropriate amounts of Li_2MoO_4 (99+%), MoO_2 (99%), and MoO_3 (99.9995%) were pressed into rods, sealed in evacuated quartz tube, and heated in a three-zone tube furnace. The temperature controllers were collectively programmed to optimize the growth. The final products appeared as purple platelets, with typical dimensions $\sim 3 \times 1 \times 0.3$ mm³; they were separated from the flux by ultrasonic treatment in alternately diluted hydrochloric acid and distilled water. The single phase nature of the samples was confirmed by x-ray powder diffraction.

The resistivity, heat capacity, and susceptibility (M/H) of $\text{Li}_{0.9}\text{Mo}_6\text{O}_{17}$ were checked (Fig. 1) and compared with previous reports.^{1,3} The b -axis resistivity of $\text{Li}_{0.9}\text{Mo}_6\text{O}_{17}$ was measured between 2 and 300 K by the standard four-probe technique, and it clearly displays the 25 K metal-insulator transition [Fig. 1(a)]. The qualitative temperature dependence of the resistivity is consistent with the previous results, although it is lower by a factor of 6.¹

The heat capacity of a 0.96 mg crystal was measured near 25 K using a sensitive ac-calorimetric technique, described in detail elsewhere.³⁹ Oscillating power was supplied with light chopped at a frequency (22.5 Hz) between the external and internal thermal relaxation rates, and the oscillating temperature, inversely proportional to the heat capacity of the sample and its addenda, was measured. A black PbS film was evaporated on the surface so that the absorbed power was independent of temperature; since the absorbed power was not known, the specific heat was normalized, after correcting for the small (few percent) addendum contribution, to the value at 39 K reported in Ref. 3.

The behavior of our specific-heat data is similar to that reported in Ref. 3, but the anomaly near 25 K is much smaller. The difference is likely a consequence of our increased precision. As mentioned above, the authors of Ref. 3 interpreted this broad peak in specific heat to signify a CDW transition (with most of the Fermi surface lost at the transition), but it is usual for specific-heat anomalies at CDW transitions to be much sharper and range in magnitude from their

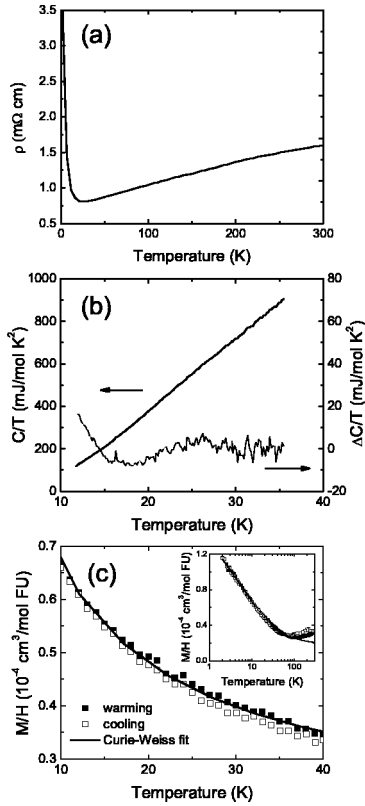


FIG. 1. (a) dc resistivity of $\text{Li}_{0.9}\text{Mo}_6\text{O}_{17}$ along the b axis. (b) Heat capacity of $\text{Li}_{0.9}\text{Mo}_6\text{O}_{17}$, plotted as C/T vs T . The bottom line shows $\Delta C/T$ obtained by subtracting a straight line from the C/T data in the vicinity of the 25 K transition. (c) Close-up view of the susceptibility (M/H) of $\text{Li}_{0.9}\text{Mo}_6\text{O}_{17}$ near the 25 K metal-insulator transition. Closed (open) symbols represent the susceptibility data taken with increasing (decreasing) temperature. The inset displays the susceptibility (M/H) of $\text{Li}_{0.9}\text{Mo}_6\text{O}_{17}$ between 2 and 300 K. The solid line in both the main panel and the inset shows a Curie-Weiss susceptibility fit to the data.

mean-field value, $\Delta C/T = 1.4\Delta\gamma$, where γ is the Sommerfeld coefficient in the electronic specific heat, to a few times greater than this (e.g., in quasi-one-dimensional materials with large fluctuations). For example, in well-known quasi-one-dimensional blue bronze ($\text{K}_{0.3}\text{MoO}_3$), $\Delta C/T \sim 4.2\Delta\gamma$.⁴⁰ From the scatter in our data for $\text{Li}_{0.9}\text{Mo}_6\text{O}_{17}$ shown in Fig. 1(b), we estimate an upper limit to an anomaly of $\Delta C/T < 3$ mJ/mol K². Then from the low-temperature value of $\gamma_0 \sim 6$ mJ/mol K² of Ref. 3, our results suggest that less than 25 % of the Fermi surface is destroyed if the transition is mean field, with the fraction a few times smaller than this if there are quasi-one-dimensional fluctuations.

The susceptibility $M(T)/H$ of Li purple bronze was determined in the temperature range $T = 2$ –300 K, with a magnetic field $H \parallel c$ axis, i.e., normal to the growth plane of the crystals. The sample (32 mg) consisted of ~ 10 small crystals, glued on a thin Mylar disk. The measurements were conducted in a Quantum Design MPMS-7 SQUID-based magnetometer, in a fixed magnetic field $H = 10$ kOe = 1 T. As noted below, the magnetic moment of the Li purple bronze was small and consequently the background of the

mounting disk and materials were carefully accounted for in separate measurements. The resulting susceptibility M/H (in units of cm³/mole formula unit) is shown versus T on a log scale in the inset to Fig. 1(c). The main panel of Fig. 1(c) shows an expanded plot of the susceptibility at low temperatures. Our measured susceptibility is smaller than that reported previously.¹ Experimentally, several different mechanisms can contribute to the observed susceptibility: Pauli paramagnetism, Landau diamagnetism, core diamagnetism, and perhaps an orbital paramagnetism (all of which are temperature independent at sufficiently low temperature), and a Curie-Weiss contribution due to local moments. The solid line shows a Curie-Weiss susceptibility $\chi = \chi_0 + C/(T + \Theta)$ fitted to the data for $T \leq 100$ K. The Curie constant C corresponds to a concentration of $\sim 2 \times 10^{-3}$ per mole formula unit of local moments with $S = 1/2$, $g = 2$, i.e., ~ 360 ppm relative to Mo content. The Θ value is antiferromagnetic in sign, with $\Theta = 6$ K and $\chi_0 \sim +0.18 \times 10^{-4}$ cm³/mol formula unit.

Most notable is an absence of any discernable anomaly in the region near 25 K. Aside from the Curie-Weiss-like term, the remaining (nominally temperature independent) term χ_0 is rather small. This is due to a near-cancellation of the Pauli, Landau, orbital, and core terms; for example, we estimate the core contribution⁴¹ alone to be -2.7×10^{-4} cm³/mol formula unit, which is much larger in magnitude than χ_0 . While this cancellation means that one cannot reliably isolate the Pauli susceptibility, $\chi_{Pauli} \propto \gamma$, it also makes the susceptibility highly sensitive to any change in χ_{Pauli} . Indeed, for a CDW transition, one expects a change in the Pauli susceptibility $\Delta\chi_{Pauli} \sim \Delta N(\epsilon_F)\mu_B^2$ with $\Delta N(\epsilon_F)/N(\epsilon_F) = \Delta\gamma/\gamma_0$, where $N(\epsilon_F)$ is the electronic density of states and γ is the Sommerfeld coefficient in the electronic specific heat. From the data in Fig. 1(c) and the absence of any discernable anomaly in χ near 25 K, it is clear that the change in γ and N is less than a few percent near the metal-insulator transition. Hence, both the specific-heat and susceptibility data suggest that the resistivity increase at 25 K does not signify a thermodynamic anomaly.

For reflectance experiments, the crystals were cleaved along the ab plane, resulting in a smooth surface. Near normal polarized reflectance measurements were carried out over a wide energy range with a series of Fourier transform and scanning grating spectrometers, covering the energy range from 6 meV to 5.6 eV (50 – $45\,000$ cm⁻¹). The resolution was 2 cm⁻¹ in the far and middle infrared and 2 nm in the near infrared, visible, and near ultraviolet. The principal axes of $\text{Li}_{0.9}\text{Mo}_6\text{O}_{17}$ were chosen as those displaying the greatest optical anisotropy. Standard wire grid, film, and prism polarizers were used over the full frequency range, providing directional selection along the chosen optical axes, which correspond to parallel and perpendicular to b (which is close to the a axis), respectively. Variable temperature experiments were carried out at 10, 50, 100, 200, and 300 K using an open-flow liquid helium cryostat and temperature control system. In order to obtain the absolute reflectance, we corrected for the response of the aluminum reference mirror as well as for scattering effects of the sample. The latter was done by evaporating a thin aluminum film on the sample

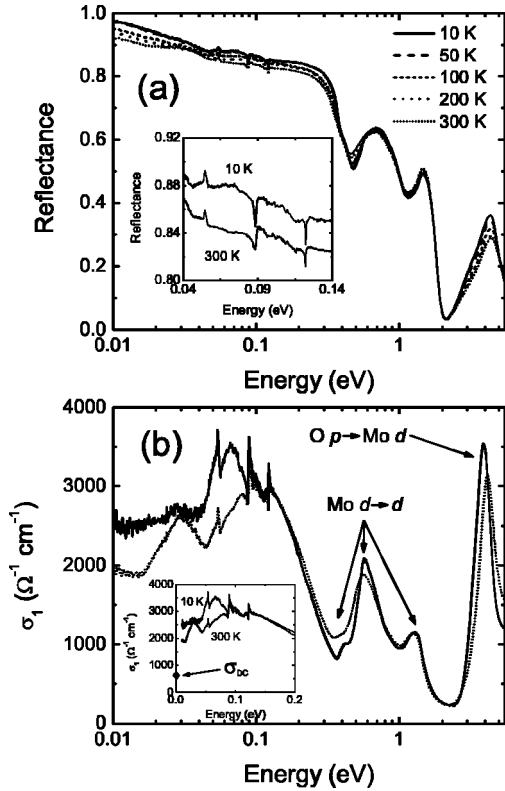


FIG. 2. (a) Reflectance spectra of $\text{Li}_{0.9}\text{Mo}_6\text{O}_{17}$ at 10, 50, 100, 200, and 300 K along the b axis. The inset shows a close-up view of the partially screened middle-infrared vibrational modes. (b) Optical conductivity of $\text{Li}_{0.9}\text{Mo}_6\text{O}_{17}$ at 10 (solid line) and 300 K (dotted line) along the b axis. The intermediate temperature optical conductivity spectra are not shown for clarity. Assignments for the electronic excitations are indicated in this panel. The inset displays a close-up view of the low-energy optical conductivity vs energy on a linear scale. The room-temperature dc conductivity ($\sim 625 \Omega^{-1} \text{cm}^{-1}$) is also indicated.

and using it as a reference. The optical conductivity spectra were obtained via Kramers-Kronig analysis of the reflectance spectra.⁴² Standard peakfitting techniques were used, as appropriate.

III. RESULTS AND DISCUSSION

A. Optical properties of $\text{Li}_{0.9}\text{Mo}_6\text{O}_{17}$ along the b axis

Figure 2 displays the variable temperature polarized reflectance and calculated optical conductivity of $\text{Li}_{0.9}\text{Mo}_6\text{O}_{17}$ along the b axis. The spectra are typical of a quasi-one-dimensional conductor, with high reflectance at low energies, partially screened vibrational features, a sharp plasma edge, and broad electronic excitations at higher energy. Overall, these features become more pronounced in the low-temperature response.

The low-energy optical conductivity of $\text{Li}_{0.9}\text{Mo}_6\text{O}_{17}$ displays an unusual mobile carrier response along the b axis. It is not Drude-like at any temperature that we investigated. Instead, it exhibits unconventional behavior, suggesting partial localization superimposed upon a large residual conductivity. The localization can be more clearly seen in the inset

of Fig. 2, where the plot has a linear (rather than logarithmic) scale. Note that this behavior is different from that reported previously, where a Drude response was used to describe the low-energy electrodynamics of $\text{Li}_{0.9}\text{Mo}_6\text{O}_{17}$.²⁰ The peak near 0.1 eV is reminiscent of a bound-carrier excitation, and the optical conductivity drops below this energy. As σ_1 approaches zero energy, the results are in overall reasonable agreement but somewhat higher than the dc conductivity ($\sim 625 \Omega^{-1} \text{cm}^{-1}$). Despite clear carrier localization and the decrease in σ_1 below 0.1 eV, there is no evidence for an optical gap. Possibly, one could argue for a pseudogap-type structure in the far infrared, based upon the aforementioned evidence for carrier localization. However the residual conductivity of $\text{Li}_{0.9}\text{Mo}_6\text{O}_{17}$ is substantial, $\geq 2000 \Omega^{-1} \text{cm}^{-1}$, at all temperatures.⁴³ Note that selected photoemission measurements predict a gap near 80 meV,¹⁷ in the vicinity of the drop in σ_1 . Our spectroscopic measurements show only that there are important localization effects at this energy scale, although it is likely that these two effects are related. With decreasing temperature, spectral weight moves from the higher-energy tail of this structure ($\sim 0.1\text{--}0.3$ eV) to lower energy (below ~ 0.1 eV). This change in spectral weight is discussed in detail below, but it is worth noting here that, based on the shift of oscillator strength and the reduced value of σ_{dc} below 25 K, the carriers are slightly more localized at low temperatures. A non-Drude line shape with suppressed conductivity near zero energy has been observed in many correlated electron systems including high- T_c cuprates, organic superconductors, heavy fermion materials, bronzes, and manganites.^{44–53} Even though the exact mechanism responsible for the suppression of the Drude peak is still not clearly understood, it is widely thought that electron interactions and localization effects due to the reduced dimensionality, electron-lattice interaction (polaron defects), or disorder play an important role.^{45,52–55}

In order to further investigate the temperature dependence of the unconventional mobile carrier response of $\text{Li}_{0.9}\text{Mo}_6\text{O}_{17}$ along b , we analyze the low-energy oscillator strength using the partial sum rule, where the spectral weight is defined as

$$N_{eff} \left(\frac{m}{m^*} \right) = \frac{2mV_{cell}}{\pi e^2} \int_0^E \sigma_1(E') dE'.$$

Here, N_{eff} is the effective number of electrons participating in optical transitions below the cutoff energy, and e , m , m^* , and V_{eff} are the free-electron charge, free-electron mass, effective mass, and volume of one formula unit, respectively.

Figure 3 displays the oscillator strength sum rule for $\text{Li}_{0.9}\text{Mo}_6\text{O}_{17}$ along the b axis at 10 and 300 K (in the energy range from 0.006 to 1 eV). The inset of Fig. 3 shows the temperature dependence of the spectral weight below the 0.35 eV cutoff energy, as indicated by the dashed line in Fig. 3. This rendering provides an opportunity to focus on the low-energy portion of the spectral response. The results imply that either (1) the effective mass of $\text{Li}_{0.9}\text{Mo}_6\text{O}_{17}$ decreases on approach to the 25 K metal-insulator transition, or (2) the effective number of carriers participating in the low-energy, localized excitation increases with decreasing tem-

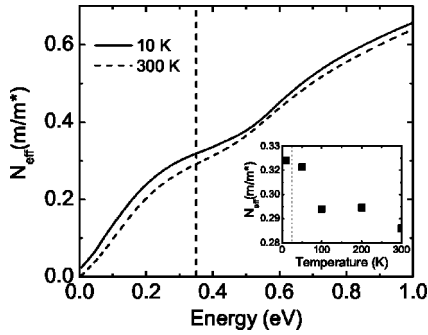


FIG. 3. Optical sum rule for $\text{Li}_{0.9}\text{Mo}_6\text{O}_{17}$, evaluated along the b axis at 10 (solid line) and 300 K (dashed line). The vertical dashed line indicates the cutoff frequency chosen for the variable temperature analysis in the inset. The inset displays the spectral weight [$N_{eff}(m/m^*)$] below the 0.35 eV cutoff energy as a function of temperature. The 25 K metal-insulator transition temperature is indicated by a vertical line in this panel.

perature. Option (2) is ruled out by previous thermopower and Hall-effect data, which show a decrease in the number of carriers below 25 K.¹⁹ Assuming that the unusual low-energy spectral response is attributable to mobile carriers, the oscillator strength variation is consistent with a change in effective mass at the 25 K metal-insulator transition. Since $1/m^* \sim \partial^2 \epsilon(k) / \partial k^2$, this result can be interpreted as a small increase in the curvature of the Fermi surface with decreasing temperature.

Despite the overall high conductivity of $\text{Li}_{0.9}\text{Mo}_6\text{O}_{17}$, we observe a number of weak vibrational features along the b direction. A close-up view of these modes is shown in the inset of Fig. 2(a). The 54, 89, and 123 meV (437, 720, and 988 cm^{-1}) modes are assigned as Mo-O stretching motions. Within our sensitivity, the temperature dependence of these features is limited. In the previous report,²⁰ the b -axis vibrational modes of $\text{Li}_{0.9}\text{Mo}_6\text{O}_{17}$ were fully screened.

Broad electronic excitations are observed at 0.42, 0.57, 1.3, and 3.9 eV in the b -polarized optical conductivity spectrum of $\text{Li}_{0.9}\text{Mo}_6\text{O}_{17}$ (Fig. 2). Based on recent electronic structure calculations^{10,30,31} and photoemission work,¹² we assign the 0.42, 0.57, and 1.3 eV bands as Mo $d \rightarrow d$ transitions. Although $\text{Li}_{0.9}\text{Mo}_6\text{O}_{17}$ is a mixed-valence compound (with Mo^{5+} and Mo^{6+} sites), the large Mo-Mo distances preclude substantial intensity in charge-transfer excitations. Thus, the three electronic excitations below 2 eV correspond to localized intraatomic transitions. The intense band at 3.9 eV is attributed to O $p \rightarrow \text{Mo } d$ charge-transfer excitations. Note that these assignments are different from those reported in the previous optical study.²⁰ With decreasing temperature, the Mo $d \rightarrow d$ excitations display the usual blue shifting, whereas the O $p \rightarrow \text{Mo } d$ charge-transfer band red shifts at low temperature.

B. Optical properties of $\text{Li}_{0.9}\text{Mo}_6\text{O}_{17}$ perpendicular to the b axis

Figure 4 shows the reflectance and optical conductivity of $\text{Li}_{0.9}\text{Mo}_6\text{O}_{17}$ polarized perpendicular to the b axis (close to the a direction) at 10 and 300 K. The strong anisotropy be-

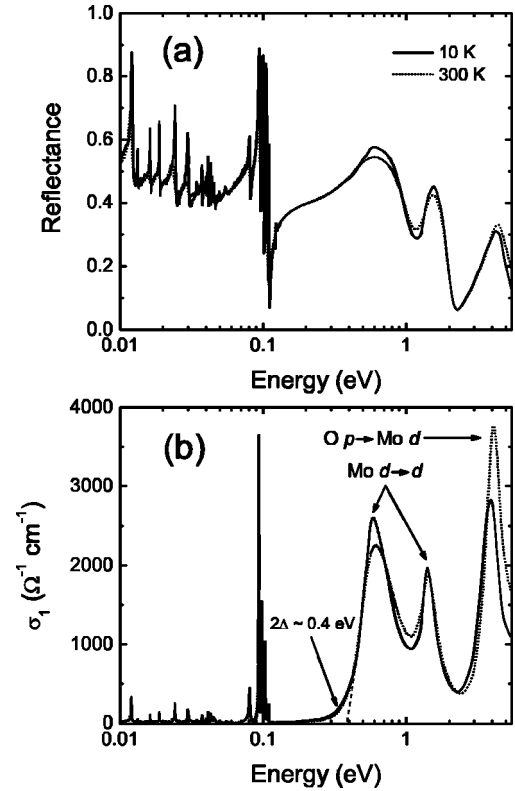


FIG. 4. (a) Reflectance and (b) optical conductivity of $\text{Li}_{0.9}\text{Mo}_6\text{O}_{17}$ polarized perpendicular to the b axis at 10 (solid line) and 300 K (dotted line). We assign the electronic excitations and the optical gap as indicated in the lower panel.

tween the $E \parallel b$ and $E \perp b$ spectra demonstrates that $\text{Li}_{0.9}\text{Mo}_6\text{O}_{17}$ is a quasi-one-dimensional conductor from the dynamics point of view, consistent with the transport properties. However, we find that the optical anisotropy is $\sim 100:1$ in the far infrared, substantially larger than that predicted from dc values (10:1).¹ This result indicates that Li purple bronze is, from an optical-properties point of view, much more one dimensional than previously anticipated. In the $\perp b$ polarization, the material displays a semiconducting response characterized by medium ($\sim 50\%$) reflectance and strong unscreened vibrational features in the infrared. Using a linear extrapolation of the leading edge of the first absorption band in σ_1 to zero conductivity, we extract an optical gap 2Δ of ~ 0.4 eV. The electronic structure of $\text{Li}_{0.9}\text{Mo}_6\text{O}_{17}$ in the $\perp b$ polarization is quite similar to that along the chains. We assign the two broadbands centered at 0.6 and 1.4 eV as Mo $d \rightarrow d$ transitions, counterparts of the 0.57 and 1.3 eV bands of similar origin in the b direction. These bands sharpen at low temperatures. Interestingly, the lowest-energy (0.42 eV) Mo $d \rightarrow d$ excitation observed in the $E \parallel b$ spectra is not apparent in the $E \perp b$ response, indicating the anisotropic nature of the lowest excited state of molybdenum d electrons in $\text{Li}_{0.9}\text{Mo}_6\text{O}_{17}$. We assign the 4.1 eV band as an O $p \rightarrow \text{Mo } d$ charge-transfer excitation. Upon cooling, the 4.1 eV charge-transfer band red shifts slightly and displays a significant decrease in oscillator strength.

Close-up views of the infrared reflectance and optical conductivity of $\text{Li}_{0.9}\text{Mo}_6\text{O}_{17}$, polarized in the $\perp b$ direction,

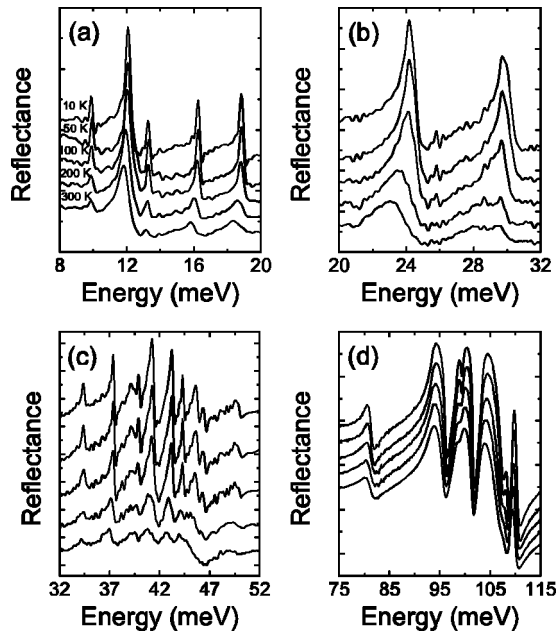


FIG. 5. Close-up view of the variable temperature reflectance of $\text{Li}_{0.9}\text{Mo}_6\text{O}_{17}$, polarized perpendicular to the b axis. The curves have been offset for clarity.

are shown in Figs. 5 and 6. The vibrational modes display substantial temperature dependence, different from the previous result.²⁰ The effect is particularly evident in Figs. 5(b) and 6(b). This observation demonstrates that the lattice of $\text{Li}_{0.9}\text{Mo}_6\text{O}_{17}$ is not perfectly rigid. Detailed mode assignment is difficult due to the low (monoclinic) symmetry and six independent Mo sites per unit cell.³⁴ Moreover, the Mo-O bond lengths range from 1.718 to 2.147 Å,³⁴ resulting in Mo-O stretching modes of the MoO_6 and MoO_4 building block units that span a wide energy range. This broadening causes the superposition of low-energy stretching modes with high-energy bending modes, as indicated by the rich spectrum between 32 and 52 meV [Fig. 5(c)]. Despite this overlap, we can make a few general assignments, as follows. Because of their short bond lengths, the higher-energy modes are related to the stretching motions of molybdenum and nonsharing oxygen atoms in the MoO_4 tetrahedra. Other strong modes shown in the range 75–115 meV are due to Mo-O stretching of the octahedra. The spectrum in Fig. 5(c) contains low-energy Mo-O stretching, O-Mo-O bending, and the vibration of lithium atoms in the large vacant site surrounded by MoO_6 octahedra and MoO_4 tetrahedra. The lowest-energy mode near 12 meV is possibly due to an external lattice motion. Close-up views of the optical conductivity in this range are shown in Fig. 6.

It is well known that vibrational spectroscopy can be a sensitive, indirect indicator of a lattice distortion and concomitant charge disproportion. The clear vibrational structure in the $\perp b$ response of $\text{Li}_{0.9}\text{Mo}_6\text{O}_{17}$ therefore provides an independent opportunity to search for evidence of a structural change at the 25 K metal-insulator transition. To this end, we closely examined the temperature dependence of the vibrational modes of $\text{Li}_{0.9}\text{Mo}_6\text{O}_{17}$ (Figs. 5 and 6). As discussed previously, if the 25 K transition is driven by a CDW

instability, a lattice distortion is expected. Our results show that the majority of vibrational modes display the usual low-temperature behavior: sharpening and blue shift with decreasing temperature. However, within the sensitivity of our measurements, we are unable to detect a substantial change in any vibrational mode through the 25 K metal-insulator transition. The 99.5 meV Mo-O stretching mode is the most likely candidate to violate this general conclusion, and we show an enlarged view of this mode and an analysis of its oscillator strength trends in the inset of Fig. 6(d). Unlike the other vibrational modes, the oscillator strength of the 99.5 meV feature [peak 2 in the inset of Fig. 6(d)] decreases with decreasing temperature. Its integrated area is plotted in comparison with the adjacent feature (peak 1), which shows normal temperature dependence.

There are many examples in the literature where both variable temperature x-ray and infrared spectroscopy have been used to investigate the microscopic details of transitions with small lattice distortions.^{56–64} Comparison of the size of the lattice distortion as measured by x-ray scattering with the infrared signature of model compounds therefore provides a way to establish an upper bound on the size of any lattice distortion in $\text{Li}_{0.9}\text{Mo}_6\text{O}_{17}$. As the first inorganic spin-Peierls material, CuGeO_3 has been extensively investigated, making it an excellent model compound for our purposes. Here, the lattice constants change by $\sim 0.004\%$ just below the 14 K spin-Peierls transition temperature.⁵⁶ Concomitant formation of zone-folding modes is observed in the infrared ($< 0.5\%$ change in reflectance) as well.^{57,58} Considering the size of the fine structure apparent in the vibrational spectrum of CuGeO_3 , the x-ray and infrared results on other model materials with incommensurate CDW distortions (blue bronze, tungsten bronzes, and TTF-TCNQ),^{19,44,65–69} as well as the typical noise level of our measurements, we estimate that any lattice distortion in $\text{Li}_{0.9}\text{Mo}_6\text{O}_{17}$ is very small, on the order of $\leq 0.001\%$ change in the lattice constants. This estimate is consistent with the heat capacity and susceptibility results, which suggest that if the 25 K transition is due to a CDW distortion, only a few percent of the Fermi surface is involved in the nesting.

IV. CONCLUSION

We report the polarized reflectance and optical conductivity of the quasi-one-dimensional conductor $\text{Li}_{0.9}\text{Mo}_6\text{O}_{17}$ at temperatures above and below the 25 K metal-insulator transition. Our results differ from those of the previous optical investigation in several important ways. At low energy, the b -polarized optical conductivity displays an unusual (non-Drude) mobile carrier response, as well as partially screened vibrational modes. No charge-density wave gap opens below the metal-insulator transition temperature, although the optical conductivity does decrease in the vicinity of the predicted gap, a sign of electronic localization. σ_1 displays substantial residual conductivity underneath this feature. Taken together, these results show that the low-energy dynamics of Li purple bronze are unusual. It is an open question as to how such a localized material becomes a superconductor at base temperatures. Likely, there is a small fraction of the Fermi sur-

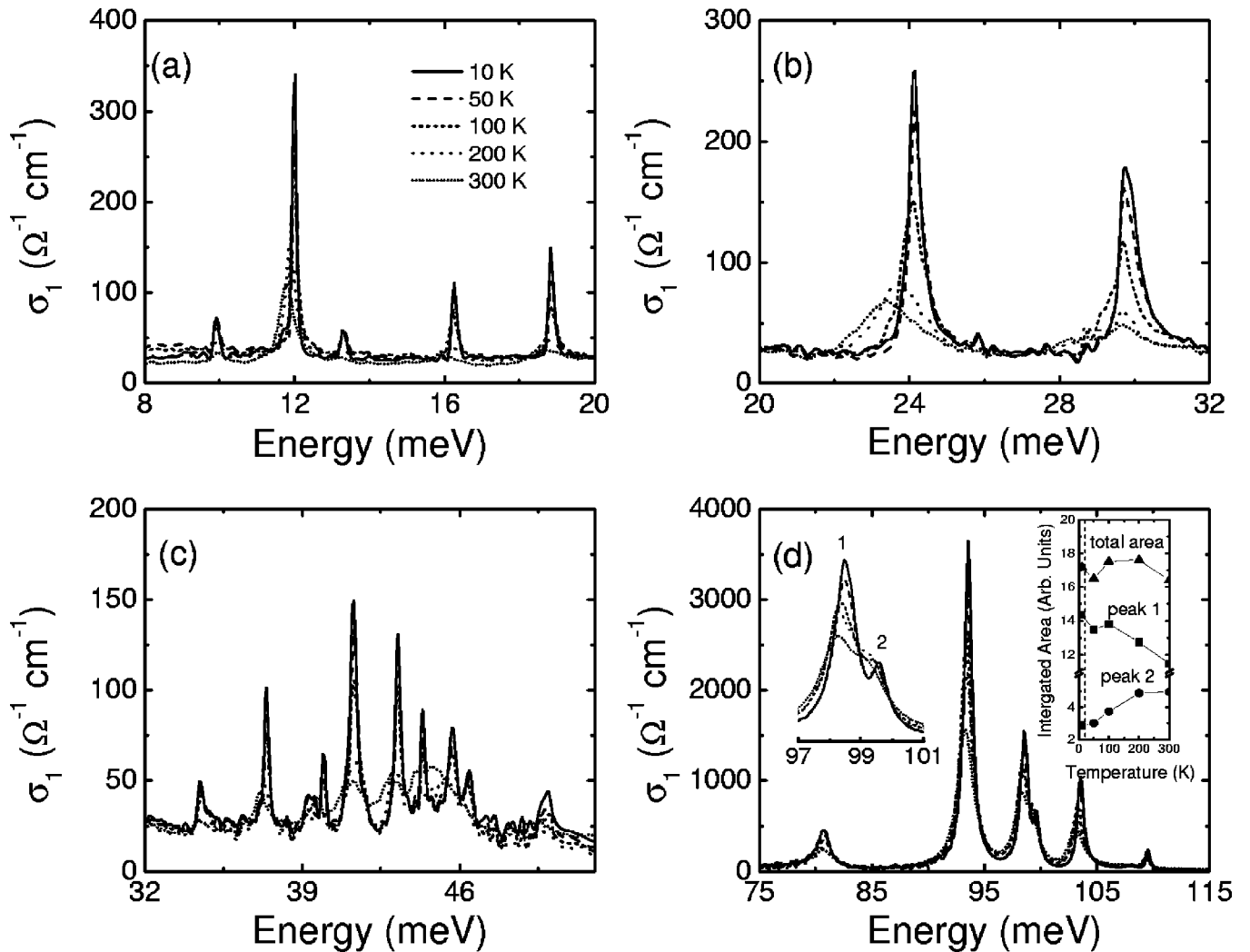


FIG. 6. Close-up view of the variable temperature optical conductivity of $\text{Li}_{0.9}\text{Mo}_6\text{O}_{17}$, polarized perpendicular to the b axis. The insets in panel (d) show a magnified view of the modes near 99 meV as well as the integrated area of these features vs temperature.

face that is not localized and is able to support low-temperature superconductivity. Recent electronic structure and photoemission results motivate us to reassign the broad electronic structures near 0.42, 0.57, and 1.3 eV as Mo $d \rightarrow d$ transitions, and we attribute the peak near 4 eV to an O $p \rightarrow \text{Mo } d$ charge-transfer band. The optical spectra of $\text{Li}_{0.9}\text{Mo}_6\text{O}_{17}$ perpendicular to the b axis display semiconducting behavior, with an optical gap of ~ 0.4 eV, rich vibrational structure, and a series of electronic excitations that are similar to those along b . These vibrational modes have substantial temperature dependence, sharpening, and blue shifting with decreasing temperature. We therefore conclude that the lattice of $\text{Li}_{0.9}\text{Mo}_6\text{O}_{17}$ is not completely rigid, meaning that there is weak temperature dependence to the infrared spectrum. However, within the sensitivity of our measurements, we find no obvious change in the vibrational spectra through the 25 K metal-insulator transition. This result suggests that if the 25 K transition is driven by a charge-density wave mechanism, the lattice distortion is quite small. Comparison with model compounds, where both high-quality x-ray and vibrational-properties data are available, allows us

to set an upper bound on any distortion in Li purple bronze as less than $\sim 0.001\%$. In addition, studies of the heat capacity and magnetic susceptibility indicate that there is no thermodynamic anomaly at the 25 K metal-insulator transition. Taken together, these results point toward localization as the dominant effect in this material.

ACKNOWLEDGMENTS

Financial support from the Materials Science Division, Basic Energy Sciences at the U.S. Department of Energy (Grant No. DE-FG02-01ER45885) for the work at University of Tennessee, and the National Science Foundation (Grant No. DMR-0100572) for the work at University of Kentucky is gratefully acknowledged. Oak Ridge National Laboratory is managed by UT-Battelle, LLC, for the U.S. Department of Energy under Contract No. DE-AC05-00OR22725. We benefited from useful conversations with J. Allen, G.-H. Gweon, S. Satpathy, M.-H. Whangbo, and J.D. Woodward.

- ¹M. Greenblatt, W.H. McCarroll, R. Neifeld, M. Croft, and J.V. Waszczak, *Solid State Commun.* **51**, 671 (1984).
- ²W.H. McCarroll and M. Greenblatt, *J. Solid State Chem.* **54**, 282 (1984).
- ³C. Schlenker, H. Schwenk, C. Escribe-Filippini, and J. Marcus, *Physica B* **B135**, 511 (1985).
- ⁴A.M. Gabovich and A.I. Voitenko, *Low Temp. Phys.* **26**, 305 (2000).
- ⁵A.M. Gabovich, A.I. Voitenko, J.F. Annett, and M. Ausloos, *Supercond. Sci. Technol.* **14**, R1 (2001).
- ⁶Y. Matsuda, M. Sato, M. Onoda, and K. Nakao, *J. Phys. C* **19**, 6039 (1986).
- ⁷M. Sato, Y. Matsuda, and H. Fukuyama, *J. Phys. C* **20**, L137 (1987).
- ⁸M. Boujida, C. Escribe-Filippini, J. Marcus, and C. Schlenker, *Physica C* **153-155**, 465 (1988).
- ⁹C. Escribe-Filippini, J. Beille, M. Boujida, J. Marcus, and C. Schlenker, *Physica C* **162-164**, 427 (1989).
- ¹⁰M.-H. Whangbo and E. Canadell, *J. Am. Chem. Soc.* **110**, 358 (1988).
- ¹¹J.D. Denlinger, G.-H. Gweon, J.W. Allen, C.G. Olson, J. Marcus, C. Schlenker, and L.-S. Hsu, *Phys. Rev. Lett.* **82**, 2540 (1999).
- ¹²G.-H. Gweon, J.D. Denlinger, J.W. Allen, R. Claessen, C.G. Olson, H. Höchst, J. Marcus, C. Schlenker, and L.F. Schneemeyer, *J. Electron Spectrosc. Relat. Phenom.* **117&118**, 481 (2001).
- ¹³G.-H. Gweon, J.D. Denlinger, C.G. Olson, H. Höchst, J. Marcus, and C. Schlenker, *Physica B* **312-313**, 584 (2002).
- ¹⁴G.-H. Gweon, J.D. Denlinger, J.W. Allen, C.G. Olson, H. Höchst, J. Marcus, and C. Schlenker, *Phys. Rev. Lett.* **85**, 3985 (2000).
- ¹⁵G.-H. Gweon, J.W. Allen, and J.D. Denlinger, *Phys. Rev. B* **68**, 195117 (2003).
- ¹⁶K.E. Smith, K. Breuer, M. Greenblatt, and W. McCarroll, *Phys. Rev. Lett.* **70**, 3772 (1993).
- ¹⁷J. Xue, L.-C. Duda, K.E. Smith, A.V. Fedorov, P.D. Johnson, S.L. Hulbert, W. McCarroll, and M. Greenblatt, *Phys. Rev. Lett.* **83**, 1235 (1999).
- ¹⁸K.E. Smith, J. Xue, L.-C. Duda, A.V. Fedorov, P.D. Johnson, W. McCarroll, and M. Greenblatt, *Phys. Rev. Lett.* **85**, 3986 (2000).
- ¹⁹J. Dumas and C. Schlenker, *Int. J. Mod. Phys. B* **7**, 4045 (1993).
- ²⁰L. Degiorgi, P. Wachter, M. Greenblatt, W.H. McCarroll, K.V. Ramanujachary, J. Marcus, and C. Schlenker, *Phys. Rev. B* **38**, 5821 (1988).
- ²¹S. Tomonaga, *Prog. Theor. Phys.* **5**, 544 (1950).
- ²²J.M. Luttinger, *J. Math. Phys.* **4**, 1154 (1963).
- ²³F.D.M. Haldane, *J. Phys. C* **14**, 2585 (1981).
- ²⁴J. Voit, *Phys. Rev. B* **47**, 6740 (1993).
- ²⁵C.L. Kane and M.P.A. Fisher, *Phys. Rev. Lett.* **68**, 1220 (1992).
- ²⁶M. Bockrath, D.H. Cobden, J. Lu, A.G. Rinzler, R.E. Smalley, T. Balents, and P.L. McEuen, *Nature (London)* **397**, 598 (1999).
- ²⁷In the Na, K, and Tl purple bronzes, an applied magnetic field stabilizes the associated CDW states, introducing dramatic metal-insulator transitions at low temperatures (Refs. 28 and 29).
- ²⁸M.L. Tian, S. Yue, S. Li, Y. Zhang, and J. Shi, *J. Appl. Phys.* **89**, 3408 (2001).
- ²⁹M. Tian, S. Yue, and Y. Zhang, *Phys. Rev. B* **65**, 104421 (2002).
- ³⁰Z. Popovic and S. Satpathy (unpublished).
- ³¹M.-H. Whangbo (unpublished).
- ³²Grüner, *Density Waves in Solids* (Addison-Wesley, Reading, Massachusetts, 1994).
- ³³D.B. McWhan, R.M. Fleming, D.E. Moncton, and F.J. DiSalvo, *Phys. Rev. Lett.* **45**, 269 (1980).
- ³⁴M. Onoda, K. Toriumi, Y. Matsuda, and M. Sato, *J. Solid State Chem.* **66**, 163 (1987).
- ³⁵H. Vincent, M. Ghedira, J. Marcus, J. Mercier, and C. Schlenker, *J. Solid State Chem.* **47**, 113 (1983).
- ³⁶N.C. Stephenson, *Acta Crystallogr.* **20**, 59 (1966).
- ³⁷M. Ganne, M. Dion, A. Boumaza, and M. Tournoux, *Solid State Commun.* **59**, 137 (1986).
- ³⁸J.P. Pouget (unpublished).
- ³⁹M. Chung, E. Figueroa, Y.-K. Kuo, Y. Wang, J.W. Brill, T. Burgin, and L.K. Montgomery, *Phys. Rev. B* **48**, 9256 (1993).
- ⁴⁰J.W. Brill, M. Chung, Y.-K. Kuo, X. Zhan, E. Figueroa, and G. Mozurkewich, *Phys. Rev. Lett.* **74**, 1182 (1995).
- ⁴¹L.N. Mulay and E.A. Boudreaux, *Theory and Application of Molecular Diamagnetism* (John Wiley, New York, 1976), p. 306 and 307.
- ⁴²In the Kramers-Kronig analysis, the high-frequency data were extrapolated as ω^{-2} in both $E\parallel b$ and $E\perp b$ polarizations, and the low-frequency data were extrapolated to zero frequency assuming a metallic response along the b axis, and with a constant in the $\perp b$ direction.
- ⁴³It is notable that the $m=7$ tungsten bronze also displays a substantial residual conductivity, attributable to the fact that the CDW gap does not form over all parts of the Fermi surface (Ref. 44).
- ⁴⁴Z.-T. Zhu, J.L. Musfeldt, Z.S. Teweldemedhin, and M. Greenblatt, *Phys. Rev. B* **65**, 214519 (2002).
- ⁴⁵F. Gervais, *Mater. Sci. Eng., R.* **39**, 29 (2002), and references therein.
- ⁴⁶A.F. Santander-Syro, R.P.S.M. Lobo, N. Bontemps, Z. Konstantinovic, Z. Li, and H. Raffy, *Phys. Rev. Lett.* **88**, 097005 (2002).
- ⁴⁷L. Degiorgi, *Rev. Mod. Phys.* **71**, 687 (1999), and references therein.
- ⁴⁸H.J. Lee, K.H. Kim, J.H. Jung, T.W. Noh, R. Suryanarayanan, G. Dhalenne, and A. Revcolevschi, *Phys. Rev. B* **62**, 11 320 (2000).
- ⁴⁹Z.-T. Zhu, J.L. Musfeldt, H.-J. Koo, M.-H. Whangbo, Z.S. Teweldemedhin, and M. Greenblatt, *Chem. Mater.* **14**, 2607 (2002).
- ⁵⁰J. Dong, J.L. Musfeldt, J.A. Schlueter, J.M. Williams, P.G. Nixon, R.W. Winter, and G.L. Gard, *Phys. Rev. B* **60**, 4342 (1999).
- ⁵¹I. Olejniczak, J.L. Musfeldt, G.C. Papavassiliou, and G.A. Mousdis, *Phys. Rev. B* **62**, 15 634 (2000).
- ⁵²A.J. Millis, *J. Electron Spectrosc. Relat. Phenom.* **114-116**, 669 (2001).
- ⁵³K. Lee, A.J. Heeger, and Y. Cao, *Phys. Rev. B* **48**, 14 884 (1993).
- ⁵⁴N.F. Mott, in *Proceedings of the Thirty-First Scottish Universities Summer School in Physics of 1986*, edited by D.M. Finlayson (Edinburgh University Press, Edinburgh, 1986).
- ⁵⁵N.F. Mott, in *Localization 1990*, edited by K.A. Benedict and J.T. Chalker, IOP Conf. Proc. No. 108 (Institute of Physics and Physical Society, Bristol, 1990).
- ⁵⁶M.D. Lumsden, B.D. Gaulin, and H. Dabkowska, *Phys. Rev. B* **57**, 14 097 (1998).
- ⁵⁷M.N. Popova, A.B. Sushkov, S.A. Golubchik, A.N. Vasil'ev, and L.I. Leonyuk, *Phys. Rev. B* **57**, 5040 (1998).
- ⁵⁸A. Damascelli, D. van der Marel, G. Dhalenne, and A. Revcolevschi, *Phys. Rev. B* **61**, 12 063 (2000).

- ⁵⁹M. Isobe and Y. Ueda, *J. Phys. Soc. Jpn.* **65**, 1178 (1996).
- ⁶⁰Y. Fujii, H. Nakao, T. Yosihama, M. Nishi, K. Nakajima, K. Kakurai, M. Isobe, Y. Ueda, and H. Sawa, *J. Phys. Soc. Jpn.* **66**, 326 (1997).
- ⁶¹M.N. Popova, A.B. Sushkov, S.A. Golubchik, B.N. Mavrin, V.N. Denisov, B.Z. Malkin, A.I. Iskhakova, M. Isobe, and Y. Ueda, *J. Exp. Theor. Phys.* **88**, 1186 (1999).
- ⁶²B. Van Bodegom, B.C. Larson, and H.A. Mook, *Phys. Rev. B* **24**, 1520 (1981).
- ⁶³R.J.J. Visser, S. Oostra, C. Vettier, and J. Voiron, *Phys. Rev. B* **28**, 2074 (1983).
- ⁶⁴Y. Tanaka, N. Satoh, and K. Nagasaka, *J. Phys. Soc. Jpn.* **59**, 319 (1990).
- ⁶⁵C. Hess, C. Schlenker, G. Bonfait, T. Ohm, C. Paulsen, D. Dumas, Z. Teweldemedhin, M. Greenblatt, J. Marcus, and M. Almeida, *Solid State Commun.* **104**, 663 (1997).
- ⁶⁶S. Jandl, M. Banville, C. Pépin, J. Marcus, and C. Schlenker, *Phys. Rev. B* **40**, 12 487 (1989).
- ⁶⁷L. Degiorgi, B. Alavi, G. Mihaly, and G. Grüner, *Phys. Rev. B* **44**, 7808 (1991).
- ⁶⁸D.B. Tanner, K.D. Cummings, and C.S. Jacobsen, *Phys. Rev. Lett.* **47**, 597 (1981).
- ⁶⁹S. Kagoshima, T. Ishiguro, and H. Anzai, *J. Phys. Soc. Jpn.* **41**, 2061 (1976).